Journal of Alloys and Compounds 509S (2011) S334–S337

Contents lists available at ScienceDirect

Journal of Alloys and Compounds

journal homepage: www.elsevier.com/locate/jallcom

Martensitic transformation and thermal cycling effect in Cu–Co–Zr alloys

F.A. Javid[a,*], N. Mattern[a], S. Pauly[a], J. Eckert[a,b]

[a] IFW Dresden, Institut für Komplexe Materialien, Postfach 27 01 16, D-01171 Dresden, Germany
[b] TU Dresden, Institut für Werkstoffwissenschaft, D-01062 Dresden, Germany

ARTICLE INFO

Article history:
Received 2 July 2010
Received in revised form 14 January 2011
Accepted 27 January 2011
Available online 5 February 2011

Keywords:
Cu–Co–Zr
Rapid solidification
Martensitic transformation
Thermal analysis

ABSTRACT

$Cu_{50-x}Co_x Zr_{50}$ (x = 0, 0.5, 1, 2, 3, 4 and 5 at.%) alloys were cast in a cylindrical copper mold by a suction casting device. In order to investigate the thermal behavior of the as-cast rods, the samples were heated from 313 to 573 K and then cooled down to about 253 K. The structure of the samples was studied by X-ray diffraction and optical microscopy. Thermal cycling measurements were also done for alloys with 2, 3, 4 and 5 at.% cobalt. It was found that increasing the cobalt content decreases martensite (M_s) and austenite (A_s) start temperatures, while it increases the temperature region in which austenite is stable. Thermal cycling measurements revealed that by increasing the number of cycles, the austenite start temperature increases while martensite start temperature shifts to lower temperatures.

1. Introduction

Martensitic transformations (MT) are the phase transformation with a cooperative atomic movement and they are diffusionless solid–solid transition, which were the interesting point of many researches due to their unique properties such as shape memory effect and superelasticity [1]. The shape memory effect was first known in 1938 in Cu–Zn alloys and Cu–Sn alloys [2], but not widely used until 1963 when Ni–Ti alloys were studied. Among the various alloy systems studied so far, NiTi-based alloys are the most attractive materials with superior shape memory and super plastic properties [3–5]. On the other hand Cu–Zr-based quasi-binary intermetallics [6] show quite high MT temperature. As an example of Cu–Zr-based alloys, phase transformations in Cu–Zr–Ni alloy were studied by [7]. The MT in CuZr intermetallic and the twined nature of the martensite were first studied by Carvalho and Harris [8] and Nicholls et al. [9]. In Cu–Zr-based alloys, $Cu_{50}Zr_{50}$ intermetallic compound has a *B*2 structure which is stable above 988 K. Below this temperature and in the equilibrium state this phase decomposes into $Cu_{10}Zr_7$ and $CuZr_2$ phases; but rapid cooling to the temperatures lower than 413 K leads to a transformation of CuZr-*B*2 into metastable monolcinic structure. This phase has martensitic characteristics and shape memory effect [10,11]. On the other hand $Co_{50}Zr_{50}$ composition also has a simple cubic *B*2 structure which is stable at room temperature. It seems with the addition of proper amount of cobalt to CuZr, CuZr-*B*2 phase can be stabilized at room temperature. The purpose of the current paper is to investigate MT in the Cu–Co–Zr ternary system in which copper is replaced by cobalt while the atomic ratio of (Cu + Co):Zr is kept one. The effect of cobalt on the transformation temperatures is studied. Finally thermal cycling of some selected alloys is evaluated.

2. Experimental

Master alloys of $Cu_{50-x}Co_xZr_{50}$ compositions with different Co contents (x = 0, 0.5, 1, 2, 3, 4 and 5 at.%) were prepared by arc-melting using high-purity metals (99.99) of Cu, Zr and Co in a Ti-gettered argon (>99.999) atmosphere. The ingots were remelted several times in order to reach a good chemical homogeneity. Subsequently, cylindrical rods with a diameter of 3 mm were produced from the ingots by an Edmund Bühler suction casting device using a water-cooled copper mold. The transmission geometry STOE STADIP diffractometer with Mo-radiation ($K\alpha_1$) was used to identify the phases of the samples. Using Nikon EPIPHOT 300 optical microscopy the microstructure of the samples was characterized. Differential scanning calorimetery was used to investigate the martensitic transformation. These experiments were performed on a PerkinElmer Pyris differential scanning calorimeter at a constant heating and cooling rates of 5 K/min from 253 to 573 K and using graphite crucibles. In order to study the effect of thermal cycling on Cu–Co–Zr alloys, $Cu_{50-x}Co_x Zr_{50}$ compositions with x = 2, 3, 4 & 5 at.% cobalt were 3 times cycled with the mentioned DSC device and the same temperature regime.

3. Results and discussion

Fig. 1(a) shows the X-ray patterns of the samples with 0, 2 and 5 at.% cobalt. The main constituent for all Cu–Co–Zr samples is CuZr monoclinic phase with *pm-3m* space group and here we show some selected compositions. As reported in [10,11], in the as-cast situation, monoclinic structure is the main crystallographic structure for the $Cu_{50}Zr_{50}$ composition. In the X-ray pattern of the samples picks of the tow low temperature equilibrium phases (i.e. $Cu_{10}Zr_7$ and $CuZr_2$) also were found. Increasing the cobalt content to 5 at.%, the

---

* Corresponding author. Tel.: +49 351 4659 739; fax: +49 351 4659 452.
E-mail address: f.a.javid@ifw-dresden.de (F.A. Javid).

0925-8388/$ – see front matter © 2011 Elsevier B.V. All rights reserved.
doi:10.1016/j.jallcom.2011.01.186

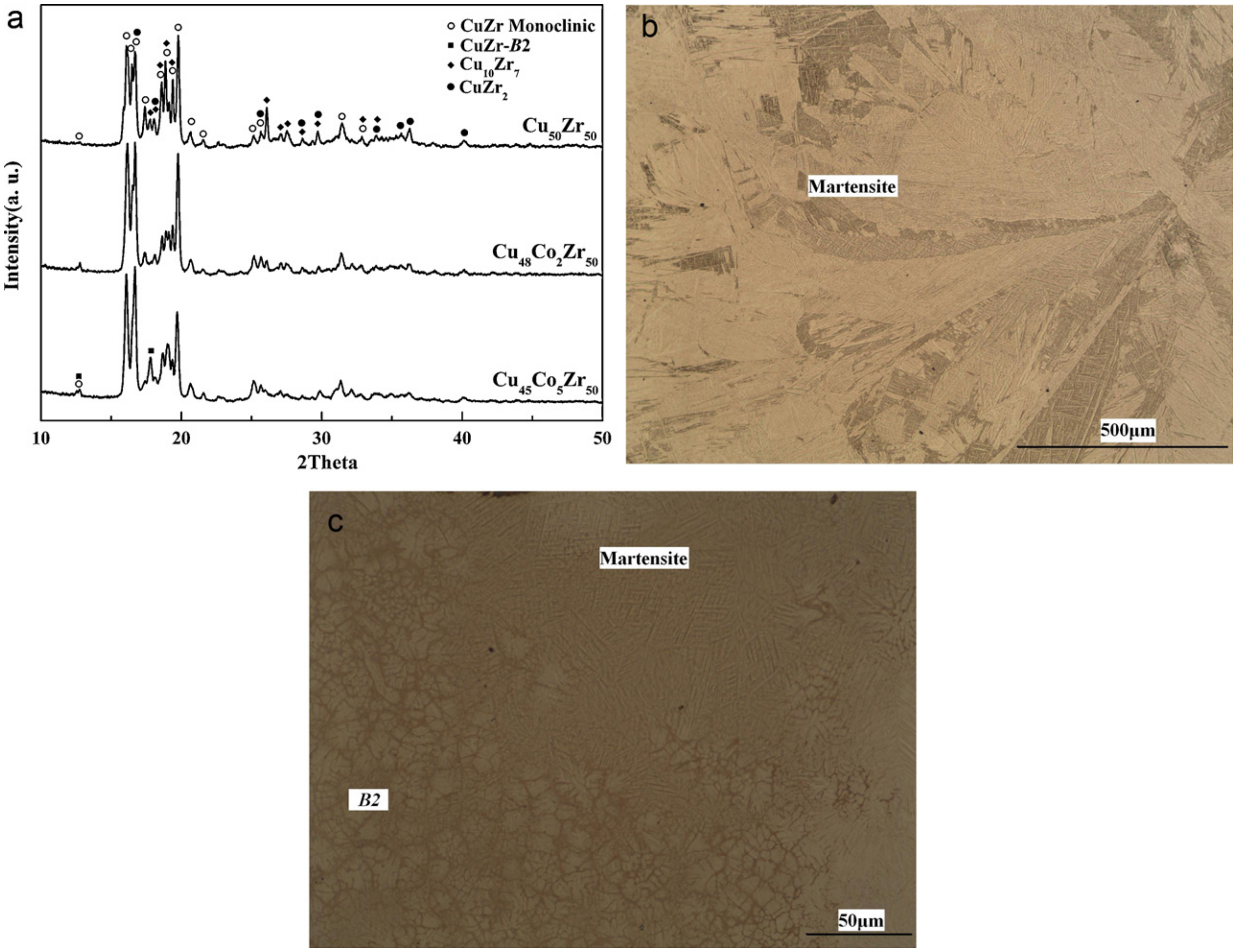

Fig. 1. (a) X-Ray patterns of $Cu_{50-x}Co_xZr_{50}$ alloys ($x = 0$, 2 and 5 at.%), micrograph of (b) $Cu_{48}Co_2Zr_{50}$ with martensite laths and (c) $Cu_{45}Co_5Zr_{50}$ which has CuZr-*B*2 phase beside martensite structure.

intensity of equilibrium phases decrease and the peak of CuZr-*B*2 phase starts to become intense mostly at around 2theta less than 18. On the other words in samples with 5 at.% cobalt CuZr-*B*2 is directly solidified from the melt and coexists with CuZr monoclinic phase. Due to 100% solubility of Co in Cu, when copper is replaced by cobalt, it forms a solid solution of (Cu, Co)Zr. Fig. 1(b and c) shows the micrographs of $Cu_{48}Co_2Zr_{50}$ and $Cu_{45}Co_5Zr_{50}$ compositions at room temperature. In $Cu_{48}Co_2Zr_{50}$ composition CuZr monoclinic is the main phase and Fig. 1(b) shows the martensite laths clearly, while by increasing the cobalt content to 5 at.%, in a higher magnification we can see the CuZr-*B*2 phase with dendritic structure coexisting with martensite.

Fig. 2(a and b) shows the heating and cooling curves of the samples respectively. For the sake of an easier comparison of all samples, all DSC curves of the heating process (from 313 to 573 K) are plotted together, and also the same for cooling curves (from 573 to 253 K). The DSC curves of Fig. 2 show an obvious martensitic transformation. For $Cu_{50}Zr_{50}$ the austenite start (A_s) and the austenite finish (A_f) temperatures are around 528 and 553 K respectively. Also for this composition martensite start (M_s) and martensite finish (M_f) temperatures are 448 and 410 K. Adding cobalt to the binary Cu–Zr system shifts the transformation temperatures. Increasing the cobalt content decreases the A_s and A_f temperatures and also M_s and M_f temperatures are decreased. For example the addition of 2 at.% cobalt shifts A_s and A_f to 485 and 503 K, respectively, while the M_s and M_f reach 410 and 387 K. It means that by adding cobalt to the binary Cu–Zr system, the temperature range in which martensite is stable decreases and austenite will be stable in a wider temperature range. With respect to the Cu–Zr phase diagram, $Cu_{50}Zr_{50}$ phase is a *B*2 type phase which is stable above 988 K and as mentioned previously decomposes to two low temperature equilibrium phases; On the other hand, in the Co–Zr binary system, $Co_{50}Zr_{50}$ intermetallic compound has a *B*2 structure which is stable at room temperature. Therefore the addition of cobalt to Cu–Zr system shifts the stability temperature of CuZr-*B*2 phase to the lower temperatures. It means that this phase is established at lower temperatures compared to $Cu_{50}Zr_{50}$ and as the X-ray results show in $Cu_{45}Co_5Zr_{50}$ composition *B*2 phase coexists with monoclinic phase in the as-cast situation. Consequently A_s and A_f appear at lower temperatures in DSC curves; also in the reverse transformation M_s and M_f start later at lower temperatures.

In order to investigate the reversibility of the transformation and to find out if any new phases are being formed, all the samples were characterized with X-Ray device after DSC. The results (not shown here) show that after DSC each composition has the same phases as it had in the as-cast mode. It means that the transformation is reversible. Fig. 3 shows the MT temperatures plotted versus cobalt content and as it was discussed the addition of cobalt shifts the martensitic transformation temperatures to lower temperatures and stabilizes the *B*2 temperature range to lower ranges. Extrapolating the data shows that by increasing the cobalt up to 7.5 at.%, M_s decreases to room temperature.

In order to investigate the effect of thermal cycling on $Cu_{50-x}Co_xZr_{50}$ ($x = 2$, 3, 4 and 5 at.% Co) compositions, 3 thermal cycles were performed on the samples. Fig. 4 shows the thermal cycling

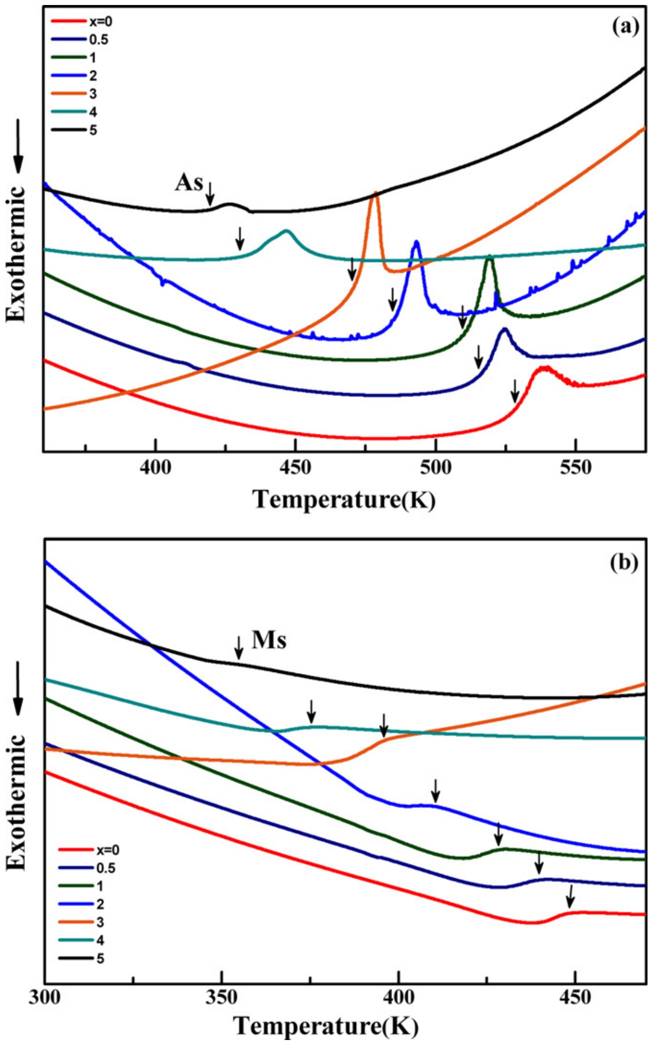

Fig. 2. DSC curves of $Cu_{50-x}Co_xZr_{50}$ alloys ($x = 0$, 0.5, 1, 2, 3, 4 and 5 at.%) upon (a) heating, (b) cooling. Heating and cooling rate 5 K/min.

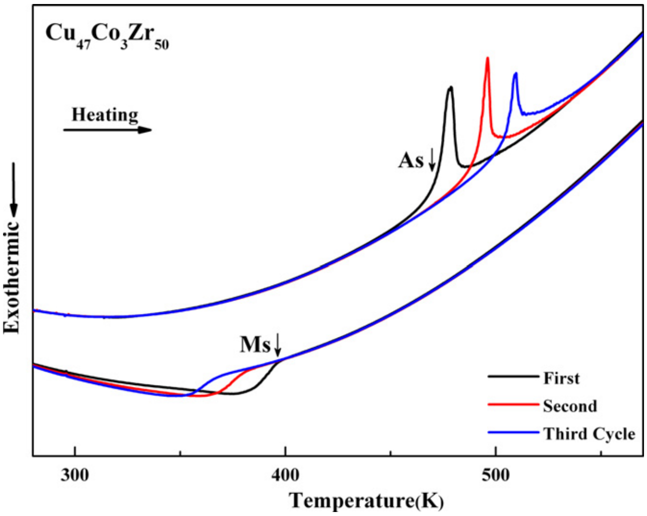

Fig. 4. Thermal cycling of $Cu_{45}Co_5Zr_{50}$ composition, Heating and cooling rate 5 K/min.

Table 1
Martensitic transformation temperatures during thermal cycling for $Cu_{50-x}Co_xZr_{50}$ ($x = 2$, 3, 4 and 5 at.% Co).

Composition	No. of cycle	$A_s \pm 5$ (K)	$A_f \pm 3$ (K)	$M_s \pm 3$ (K)	$M_f \pm 7$ (K)
$Cu_{48}Co_2Zr_{50}$	1	485	503	410	387
	2	510	519	392	376
	3	525	536	385	364
$Cu_{47}Co_3Zr_{50}$	1	470	482	396	360
	2	491	498	382	348
	3	504	511	368	–
$Cu_{46}Co_4Zr_{50}$	1	431	457	375	343
	2	446	470	359	–
	3	455	481	345	–
$Cu_{45}Co_5Zr_{50}$	1	419	434	355	338
	2	430	446	344	–
	3	437	455	335	–

curves of $Cu_{47}Co_3Zr_{50}$ as an example and all the martensitic transformation temperatures of the compositions are summarized in Table 1. As Fig. 4 shows in the reverse transformation it is tricky to determine the martensite finish temperature. This matter is more pronounced by increasing the cobalt content and also the cycling numbers. It is observed that there are some shifts in the forward and reverse transformation temperatures in all of the samples. A_s and A_f increase by increasing the number of the cycles, while M_s and M_f decrease. This effect was also observed by [12–14]. They have all attributed this effect to the changes in the structure of the parent phases (here the *B*2 phase). In fact the cyclic repetition of the transformation imposes a lot of lattice defects like dislocations and stacking faults to the structure and changes the Gibbs free energy state of the parent phases. Thus the amount of the energy needed to reach to the activation state for the beginning of the transformation will differ. This change shows itself in the form of observed shifts in transformation temperatures. It is expected that by increasing the number of cycles, the temperatures will not change considerably after a certain number of cycles due to the saturation limit of the crystals for defects [15]. The amount of lattice defects cannot increase continuously and reaches to a saturation limit. Therefore the Gibbs free energy level will reach to a certain value and will not change and as a consequence, transformation temperatures will not change considerably.

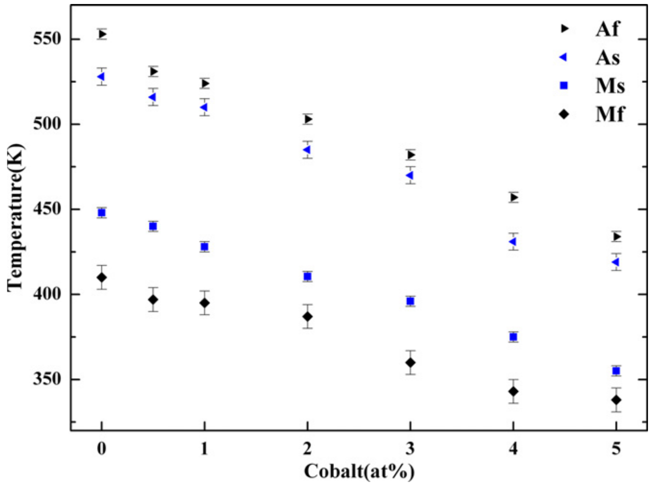

Fig. 3. Martensitic transformation temperatures versus cobalt content.

4. Conclusions

Martensitic transformation of $Cu_{50-x}Co_x$ Zr_{50} ($x = 0$, 0.5,1,2,3,4 and 5 at.%) as-cast rods was investigated. It was found that before and after the transformation the main phase is CuZr monoclinic and the transformation is reversible. Cobalt affects the martensitic transformation temperatures and shifts them to the lower temperatures. It was observed that increasing the cobalt content decreases the stability temperature range of martensite to the lower temperatures and enhance increasing the stability range of austenite. Extrapolating the data derived from the DSC curves showed that for a composition with around 7.5 at.% cobalt M_s will be around room temperature. Increasing the number of cycles in thermal cycling revealed that for a composition with a constant cobalt content, M_s and M_f decrease while A_s and A_f increase.

Acknowledgements

The authors acknowledge Dr. Stefan Roth and Seven Donath for their valuable help in performing the experiments.

Appendix A. Supplementary data

Supplementary data associated with this article can be found, in the online version, at doi:10.1016/j.jallcom.2011.01.186.

References

[1] X.B. Ren, K. Otsuka, Scripta Mater. 38 (1998) 1669–1675.
[2] A.B. Greninger, V.G. Mooradian, Trans. Am. Inst. Min. Metall. Eng. 128 (1938) 337–355.
[3] W.J. Buehler, R.C. Wiley, J.V. Gilfrich, J. Appl. Phys. 34 (1963) 1475.
[4] M. Nishida, S. Ii, K. Kitamura, T. Furukawa, A. Chiba, T. Hara, K. Hiraga, Scripta Mater. 39 (1998) 1749–1754.
[5] P.L. Potapov, A.V. Shelyakov, D. Schryvers, Scripta Mater. 44 (2001) 1–7.
[6] G. Firstov, J. Vanhumbeeck, Y. Koval, Mater. Sci. Eng. A 378 (2004) 2–10.
[7] G.S. Firstov, Y.N. Koval, J. Van Humbeeck, R. Portier, P. Vermaut, P. Ochin, Mater. Sci. Eng.: A 438–440 (2006) 816–820.
[8] E.M. Carvalho, I.R. Harris, J. Mater. Sci. 15 (1980) 1224–1230.
[9] A.W Nicholls, I.R. Harris, W. Mangen, J. Mater. Sci. Lett. 5 (1986) 217–220.
[10] Y.N. Koval, G.S. Firstov, L. Delaey, J.V. Humbeeck, Scr. Metall. Mater. 31 (1994) 799–802.
[11] Y.N. Koval, G.S. Firstov, A.V. Kotko, Scr. Metall. Mater. 27 (1992) 1611–1616.
[12] S. Miyazaki, K. Otsuka, ISIJ Int. 29 (1989) 353–377.
[13] M. Sade, E. Hornbogen, Shape Memory Effect in Fe-Mn-Si Alloys, ESOMAT 1989 - Ist European Symposium on Martensitic Transformations in Science and Technology March 9-10, 1989, Bochum, Germany. 249-256, 1989. doi:10.1051/esomat/198904010.
[14] T. Tadaki, Annu. Rev. Mater. Sci. 18 (1988) 25–45.
[15] L. Sun, W.M. Huang, J.Y. Cheah, Smart Mater. Struct. 19 (2010) 055005.